

**INTERNATIONAL JOURNAL OF CURRENT RESEARCH IN  
CHEMISTRY AND PHARMACEUTICAL SCIENCES**

(p-ISSN: 2348-5213; e-ISSN: 2348-5221)

[www.ijcrps.com](http://www.ijcrps.com)

(A Peer Reviewed, Referred, Indexed and Open Access Journal)

DOI: 10.22192/ijcrps

Coden: IJCROO(USA)

Volume 12, Issue 6- 2025

**Research Article**



DOI: <http://dx.doi.org/10.22192/ijcrps.2025.12.06.001>

**Exploring Methimazole by Spectroscopic, NLO,  
NBO, ADME Analysis, and Molecular Docking  
Studies using the DFT method.**

**Natte kavitha<sup>a\*</sup>, Munagala Alivelu<sup>b\*</sup>, Macha Bhavani<sup>c</sup>,  
Samaleti Priyanka<sup>d</sup>**

<sup>a</sup>Department of Chemistry, Government Degree College, Bhupalpally, 506169, Telangana, India,

<sup>b</sup>Department of Chemistry, Government Degree College, Gajwel, 502278, Telangana, India,

<sup>c</sup>Department of Physics, Government Degree College, Gajwel, 502278, Telangana, India,

<sup>d</sup>Department of Chemistry, Government Degree College, Huzurnagar, 508204, (Telanagana), India

*Correspondance: Email: kavithanatte2008@gmail.com*

*Correspondance: Email: munagalaalivelu@gmail.com*

Copyright © 2025. Natte kavitha et al., This is an open-access article distributed under the terms of the Creative Commons Attribution License, which permits unrestricted use, distribution, and reproduction in any medium, provided the original author and source are credited.

**Abstract**

This study was carried out to analyze Methimazole which was characterized by IR and Raman spectral analysis. The optimized molecular geometry, the vibrational wave numbers, the infrared intensities, and the Raman scattering activities were designed by using the density functional theory (DFT) B3LYP method with a 6-311++G(d,p) basis set. A detailed explanation of the vibrational spectra was assigned by the VEDA program. The stability of the molecule arising from hyper conjugative interactions and charge delocalization has been calculated using natural bond orbital analysis (NBO). The deliberated HOMO and LUMO energies show that charge transfer within the molecule. The first-order hyperpolarizability, Molecular Electrostatic Potential (MEP), and Mulliken charges were also performed. Moreover, Drug likeness properties of header molecule was predicted. Molecular docking was done to study the biological activity of the title molecule to identify the hydrogen bond and binding energy.

**Keywords:** Methimazole; DFT; Molecular docking; Drug likeness.

## 1. Introduction

Methimazole (MMI/MTZ) commercially well known as tapazole (TZ), is a heterocyclic compound widely used in the treatment of hyperthyroidism. Anti-thyroid drugs, Carbimazole, Methimazole, and Propylthiouracil, suppress the production of thyroid hormones by blocking the incorporation of oxidized iodines into tyrosine residues in the large thyroid hormone precursor molecule, thyroglobulin, which is the first step of the hormonal biosynthesis. Therefore, it has been proposed that the donor properties of anti-thyroid agents are the origin of their anti-thyroid action<sup>1-2</sup>. These anti-thyroid drugs could divert I<sub>2</sub> from the second oxidation step of iodides and consequently prevent the electrophilic substitution on the tyrosine residues of thyroglobulin by forming a stable complex with I<sub>2</sub>. These compounds, for this reason, are major drugs that are widely used clinically in the treatment of hyperthyroidism. All anti-thyroid agents contain the thiourea pharmacophore. Because of the push-pull mechanism in which the nitrogen lone pairs donate electrons to the thiocarbonyl group, this pharmacophore must possess significant electron donor properties at the sulfur atom.

MTZ is one of theazole derivatives that is extensively used in the field of inhibition of metals from corrosion<sup>3</sup>, due to its presence in a wide range of pharmaceutical formulations; the determination of MTZ is a significant area of interest. MTZ has been investigated by various methods including; electrochemical techniques, high-performance liquid chromatography, gas chromatography, fluorescence probe method, and Raman spectroscopies<sup>4,5</sup>. However, these techniques required additional derivatization procedures and were more time-consuming<sup>6</sup>. The therapeutic intake of MTZ may nevertheless have hepatotoxic effects and cause serious adverse health effects, such as vasculitis, lupus erythematosus syndrome, nephritis, and thrombocytopenia<sup>7-9</sup>. The tautomeric equilibrium of the methimazole analogous compounds has been investigated using different methods<sup>7-9</sup>.

The literature review revealed that no detailed quantum chemistry study has been carried out for the title compound. The DFT (B3LYP) method was used for theoretical calculations. We first determined the optimized structures of the Methimazole molecule by using the density functional theory. The optimized structural parameters such as bond lengths and bond angles and dihedral angles of the title molecule were determined. Molecular properties such as dipole moment, polarization, first-order hyperpolarizability, molecular electrostatic potential, and Mulliken atomic charges have been calculated for the title compound. The Natural bond orbital analysis is used to study the stability of a molecule arising from hyper conjugative interaction and charged delocalization. Drug-likeness and molecular docking studies were performed using the structure of 1NHZ protein and were discussed to establish its biological activity.

## 2. Computational techniques

In computational methods, the Gaussian 09 software program package is used<sup>10</sup>. The quantum chemical calculations were performed by the density functional theory method<sup>11</sup> with the three-parameter hybrid functional (B3) for the exchange part and the Lee-Yang-Par (LYP) correlation function with 6-311++G (d, p) basis set. The Natural bonding orbital calculations were enunciated. The NLO candidature and the hyperpolarizability of the molecule were carried out. The molecular electrostatic potential which summarizes the charge distribution of the molecule was examined to find out the nucleophilic and electrophilic regions of the compound. Auto Dock 4.2.6 is used for molecular docking study and the docked structures were visualized using Biovia discovery studio visualizer 3.5.

## 3. Results and Discussion

### 3.1. Molecular geometry

The molecular structure of the compound belongs to C<sub>1</sub> point group symmetry. The optimized

Structure parameters were calculated and listed in **Table 1**. The optimized geometric structure with the numbering of atoms of the compound is shown in **Fig. 1**. **Table 1** displays the calculated bond lengths and bond angles of the compound. There are one C-C, four C-N, five C-H, one C-S, and one S-H, in the compound. The bond length of C-S was 1.7728 Å highest among the others. The lowest bond length was 1.0722 Å observed between C1-H5. The bond length of N4-C8 is

1.4547 Å respectively. The bond length between C and S atoms is larger when it is in a single bond. The bond length between C-H atoms is smaller when the C1 atom is attached to a less electronegative atom of hydrogen. The maximum value of the bond angle was observed between C2-C1-H5 as 132.6°. The minimum dihedral angle observed between H5-C1-C2-H7 is -0.2494° respectively.

**Table 1.** Optimized geometrical parameters bond length, bond angle of the title molecule B3LYP/6-311++G (d, p).

Bond length	Value(Å)	Bond angle	Value(°)	Dihedral angle	Value(°)
C1-C2	1.3672	C2-C1-N4	105.8204	N4-C1-C2-H6	179.3892
C1-N4	1.3878	C2-N1-H5	132.6034	N4-C1-C2-H7	-0.3873
C1-H5	1.0772	N4-C1-H5	121.5753	H5-C1-C2-H6	-0.2494
C2-H6	1.0786	C1-C2-H6	128.1955	H5-C1-C2-H7	179.9741
C2-N7	1.3782	C1-C2-N7	110.571	C2-C1-N4-C3	0.4863
C3-N4	1.3677	H6-C2-N7	121.2331	C2-C2-N4C8	178.1638
C3-N7	1.3133	N4-C3-N7	112.5685	H5-C1-N4-C3	-179.826
C3-S12	1.7728	N4-C3-S12	121.4602	H5-C1-N4-C8	-2.1484
N4-C8	1.4547	N7-C3-S12	125.9711	C1-C2-N7-C3	0.1236
C8-H9	1.0916	C1-N4-C3	105.9641	H6-C2-N7-C3	-179.671
C8-H10	1.0893	C1-N4-C8	126.7404	N7-C3-N4-N1	-0.4433
C8-H11	1.0993	C3-N4-C8	127.25	N7-C3-N4-N8	-178.1052
S12-H13	1.3466	C2-N7-C3	105.0736	S12-N3-N4-C1	179.4213
		N4-C8-H9	110.0525	S12-N3-N4-C8	1.7593
		N4-C8-H11	111.2567	N4-C3-N7-C2	0.2036
		C9-C8-H10	108.4816	S12-C3-N7-C2	-179.6536
		C9-C8-H11	109.1016	N4-C3-S12-H13	174.5314
		H10-C8-H11	108.9799	N7-C3S12-H13	-5.6231
		C3-S12-H13	92.833	C1-N4-C8-H9	137.3625
				C1-N4-C8-H11	-101.5874
				C3-N4-C8-H9	-45.443
				C3-N4-C8-H11	75.6071

Å-Angstrom; °-degree.

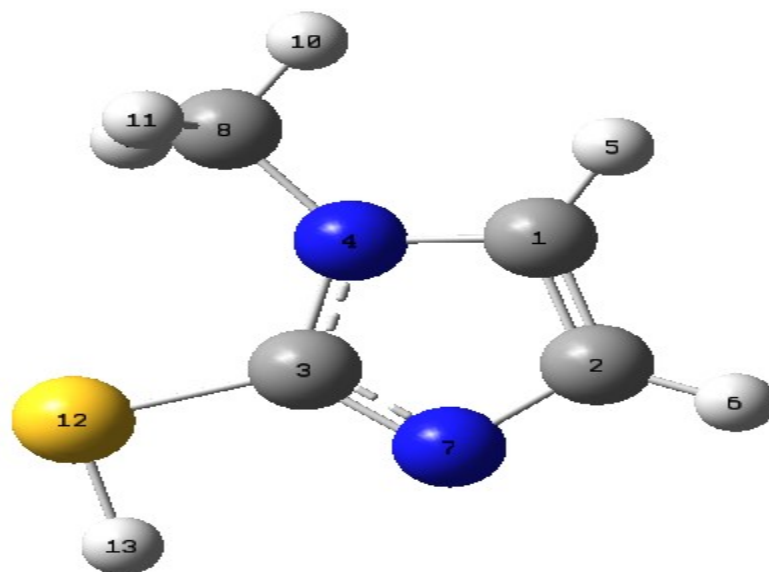


**Fig. 1.** Optimized geometric structure with atoms numbering of Methimazole molecule.

### 3.2. Vibrational analysis

The Methimazole molecule has 13 atoms with 33 (no's) normal fundamental vibrations. DFT computations was done for gas phase molecule. The basic modes of vibrations over the entire

frequency and the PED (Potential Energy distribution) assignments are values shown in **Table 2**. The Theoretical FT-IR and FT-Raman spectra of the Methimazole compound are shown in Fig. 2 and Fig. 3 respectively.

**Table 2.** Observed and calculated vibrational frequency of Methimazole compound using B3LYP method with 6-311 ++ G (d, p) basis set.

Mode	Unscaled	Scaled	IR	RAMAN	Assignments
33	3267.74	3140.30	1.44	1.27	$\nu$ CH(100)
32	3214.75	311.32	4.26	91.40	$\nu$ CH(18)
31	3134.49	3012.24	7.73	54.62	$\nu$ CH(94)
30	3098.95	2978.10	12.23	61.54	$\nu$ CH(80)
29	3036.36	2917.95	32.93	172.02	$\nu$ CH(17)
28	2691.73	2586.76	3.41	122.56	$\nu$ SH(100)
27	1538.73	1478.22	8.61	20.83	$\nu$ NC(28)
26	1513.24	1454.22	16.01	16.23	$\nu$ CC(53)
25	1500.30	1441.79	51.38	1.99	$\nu$ NC(10)
24	1489.84	1431.12	19.25	11.39	$\nu$ NC(17)
23	1450.69	1394.12	32.95	22.29	$\nu$ NC(20)
22	1406.35	1351.50	62.58	61.05	$\nu$ SC(67)
21	1361.69	1308.58	3.71	17.96	$\beta$ CNC(15)
20	1305.34	1254.43	33.37	8.37	$\beta$ HCCC(12)
19	1169.90	1124.26	3.26	4.61	$\beta$ HCC(16)
18	1156.80	1111.69	24.16	1.30	$\beta$ HCH(51)
17	1141.34	1096.83	2.17	2.83	$\beta$ HCH(10)
16	1098.69	1055.84	11.52	11.08	$\beta$ HCH(65)
15	1048.67	1007.77	3.95	1.13	$\beta$ HSC(79)

14	930.00	893.73	20.67	0.63	$\beta$ CNC(72)
13	904.70	869.42	14.53	10.10	$\beta$ CCN(29)
12	857.11	823.68	6.77	1.63	$\beta$ CNC(77)
11	713.18	685.37	34.33	1.94	$\beta$ CNC(77)
10	686.93	660.14	6.8	9.44	$\tau$ HCCN(74)
9	679.11	652.62	23.4	1.28	$\tau$ HCNC(80)
8	620.24	596.05	0.177	0.55	$\tau$ HCNC (25)
7	482.82	463.99	1.93	4.54	$\tau$ HCNC(16)
6	397.33	381.83	2.17	0.25	$\tau$ HCNC(82)
5	232.18	223.13	1.03	0.88	$\tau$ HSCN(18)
4	215.68	207.27	3.78	0.83	$\tau$ CNCN(12)
3	190.86	183.42	5.62	0.58	$\tau$ CCCN(82)
2	126.43	121.50	17.4	0.45	$\tau$ CCCN(79)
1	61.13	58.75	2.07	1.35	$\tau$ CCCN(59)

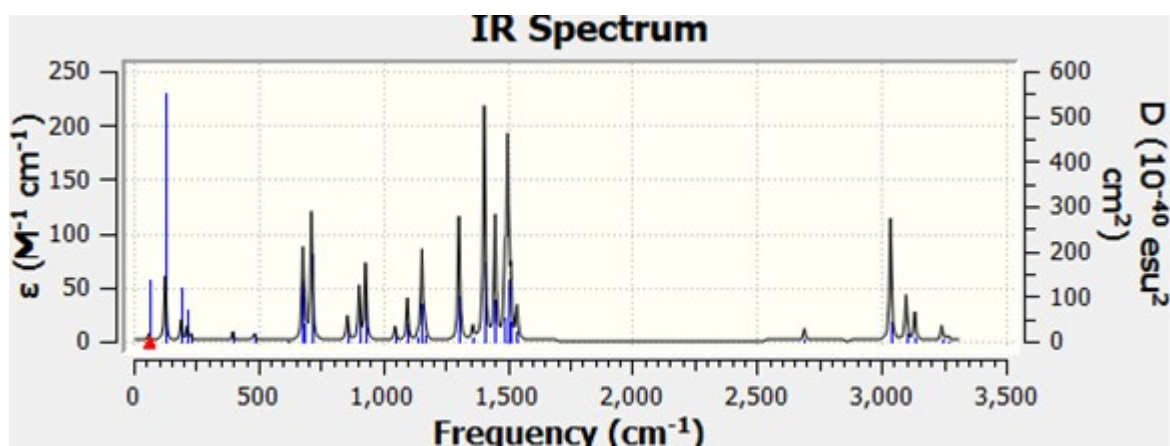


Fig. 2. FT-IR spectra of Methimazole compound (theoretical).

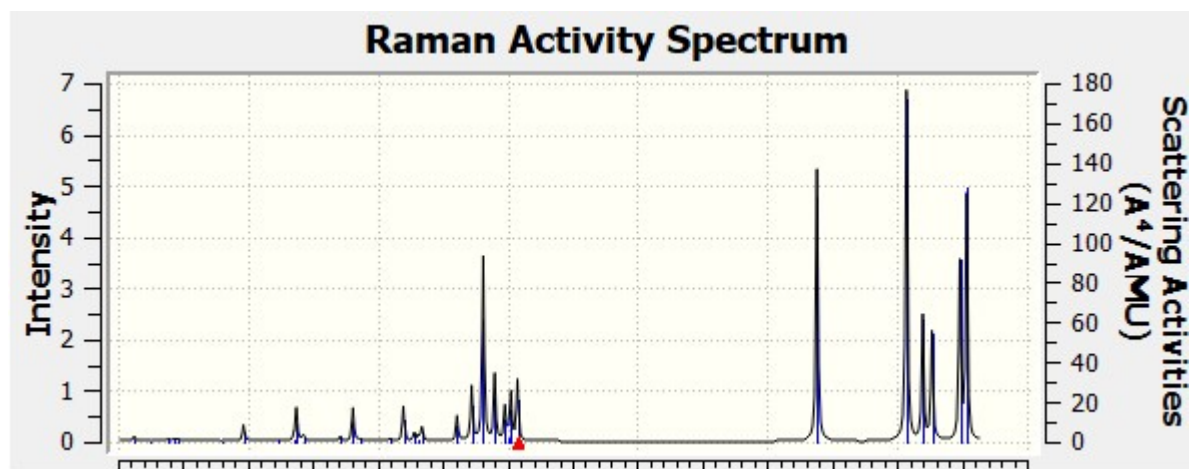


Fig. 3. FT-Raman spectra of Methimazole compound (theoretical).

### 3.2.1. S-H vibrations

The S-H stretchings are often in the 2600-2500  $\text{cm}^{-1}$ . S-H bond vibrations are found in a mode no 28 as stretching vibrations at 2691  $\text{cm}^{-1}$  with 100% PED contributions. The S-H stretching is often likely to be in the 3600-3400  $\text{cm}^{-1}$ . S-H bond vibrations are found in mode no. 33 and 32 as stretching vibrations at 3267 and 3214  $\text{cm}^{-1}$  with 100% PED contributions. The corresponding modes were observed in the FT-Raman spectrum at 3641 and 3568  $\text{cm}^{-1}$  and in the FT-IR spectra at 3681, 3674, and 3514  $\text{cm}^{-1}$ . Hence it can be proven that the theoretical values within the data obtained from the literature show the presence of SH bonding in the title molecule.

### 3.2.2. CH mode vibration

C-H stretching vibrations for organic compounds occurred in the 3100-3000  $\text{cm}^{-1}$  range<sup>12</sup>. The C-H stretching modes are predicted at (mode no. 31 and 30) 3134 and 3098 with 100, 94, and 80% PED contribution, respectively. Then, these modes are clearly assigned to the FT-IR band at 3092  $\text{cm}^{-1}$ .

### 3.2.3. CH<sub>3</sub> mode vibration

The CH<sub>3</sub> stretching modes are predicted at (mode no. 29) 3036  $\text{cm}^{-1}$ , while asymmetric stretching is observed at mode 29 and the corresponding wave numbers are 2691  $\text{cm}^{-1}$ .

### 3.2.4. C-C vibrations

The C-C stretching vibrations have a frequency range of 1650–1400  $\text{cm}^{-1}$ <sup>13</sup>. Ring stretching

vibrations are estimated to be in the 1300-1000  $\text{cm}^{-1}$  range. In the current work, C-C stretching vibrations are found at 1538 and 1513  $\text{cm}^{-1}$  for the title compound. The estimated values agree quite well with the observed results.

## 3.3 Natural bonding orbital (NBO) analysis

NBO exploration represents the achievable natural Lewis structure of the molecules under analysis. It is a convenient tool for understanding the intermolecular or intramolecular interaction, delocalization of the electron density, and hyperconjugation effects<sup>14</sup>. The second-order Fock matrix was taken for NBO analysis and the analysis has been performed using DFT. For each acceptor (*j*) and donor (*i*), the stabilization energy  $E(2)$  connected with the delocalization from *i* - *j* is calculated as,

$$E(2) = -n_{\sigma} \frac{\langle \sigma | F | \sigma \rangle^2}{\epsilon_{\sigma^*} - \epsilon_{\sigma}} = -n_{\sigma} \frac{F_{ij}^2}{\Delta E} \text{-----(1)}$$

In the present analysis, we report the significant electron acceptor, electron donor orbital, and the equivalent interacting stabilizing energies of the title compound. The most important interaction within the molecule is shown in **Table 3**. The highest association from  $\sigma$  of N4-C10 to  $\sigma^*$ C10-H12 is 62.0 kcal/mol, which observes the largest stabilization in the molecule. Another vital association from  $\pi^*$  of C3-N7 to  $\pi^*$ C1-C2 is 28.18 kcal/mol, lone pair electron on the nitrogen atom LP (1) N4 to anti-bonding of  $\pi^*$  of C3-N7 is 24.07 kcal/mol.

**Table 3.** Selective donar-acceptor interactions; based on Second-order perturbation theory analysis of Fock matrix in natural bond orbital basis.

Donor (i)	Type	ED i/e	Acceptor (j)	Type	ED i/e	<sup>a</sup> E(2) (kcal/mol)	<sup>b</sup> E(i) - E(j) (a.u)	<sup>c</sup> F(I,j) (a.u)						
C1-C2	$\sigma$	1.98879	C1-H5	$\sigma^*$	0.01335	1.84	1.18	0.042						
			C1-H6	$\sigma^*$	0.01340	1.50	1.20	0.038						
			C3-S8	$\sigma^*$	0.09363	1.04	0.90	0.028						
			N4-C10	$\sigma^*$	0.13167	2.07	1.02	0.042						
C1-C2	$\pi$	1.90066	C3-N7	$\pi^*$	0.26493	9.54	0.28	0.048						
			C10-H11	$\sigma^*$	0.06144	0.61	0.65	0.018						
C1-N4	$\sigma$	1.97889	C1-C2	$\sigma^*$	0.01482	0.92	1.36	0.032						
			C2-H6	$\sigma^*$	0.01340	2.83	1.19	0.052						
			C2-N7	$\sigma^*$	0.01817	1.13	1.10	0.031						
			C3-N4	$\sigma^*$	0.09718	0.53	1.02	0.021						
			C3-S8	$\sigma^*$	0.09363	5.08	0.89	0.061						
C1-H5	$\sigma$	1.97947	C1-C2	$\sigma^*$	0.01482	1.63	1.19	0.039						
			C2-N7	$\sigma^*$	0.01817	2.55	0.93	0.044						
			C3-N4	$\sigma^*$	0.09718	1.74	0.86	0.035						
			C10-H11	$\sigma^*$	0.06144	1.77	0.94	0.037						
C2-H6	$\sigma$	1.98686	C1-C2	$\sigma^*$	0.01482	1.29	1.17	0.035						
			C1-N4	$\sigma^*$	0.04015	2.70	0.88	0.044						
			C3-N7	$\sigma^*$	0.02732	1.51	1.11	0.037						
C2-N7	$\sigma$	1.96387	C1-C2	$\sigma^*$	0.01482	0.67	1.31	0.027						
			C1-N4	$\sigma^*$	0.04015	1.43	1.01	0.034						
			C1-H5	$\sigma^*$	0.01335	3.58	1.12	0.057						
			C3-N4	$\sigma^*$	0.09718	1.74	0.98	0.037						
			C3-S8	$\sigma^*$	0.09363	8.59	0.84	0.077						
C3-N4	$\sigma$	1.98661	C1-H5	$\sigma^*$	0.01335	2.70	1.19	0.051						
			C10-H12	$\sigma^*$	0.08768	0.52	1.09	0.022						
C3-N7	$\sigma$	1.99117	C2-H6	$\sigma^*$	0.01340	1.94	1.34	0.046						
			N4-C10	$\sigma^*$	0.13167	1.37	1.16	0.037						
			C1-C2	$\pi^*$	0.17529	10.88	0.35	0.057						
C3-N7	$\pi$	1.91455	S8-H9	$\sigma^*$	0.03208	2.83	0.53	0.035						
			C3-S8	$\sigma$	1.98178	C1-N4	$\sigma^*$	0.04015	1.27	0.99	0.032			
						C2-N7	$\sigma^*$	0.01817	3.60	1.02	0.054			
						C3-N7	$\pi^*$	0.26493	0.58	0.65	0.019			
						C3-S8	$\sigma^*$	0.09363	0.51	0.81	0.019			
						S8-H9	$\sigma^*$	0.03208	0.51	0.86	0.019			
						C10-H13	$\sigma^*$	0.09592	1.03	1.06	0.030			
						N4-C10	$\sigma$	1.97132	C1-C2	$\sigma^*$	0.01482	0.66	1.32	0.027
									C3-N7	$\sigma^*$	0.02732	1.15	1.26	0.034
									N4-C10	$\sigma^*$	0.13167	4.12	0.97	0.058
C10-H11	$\sigma^*$	0.06144	1.28	1.06	0.033									
C10-H13	$\sigma^*$	0.09592	1.75	1.09	0.040									
			C3-N7	$\sigma^*$	0.02732	0.75	1.15	0.026						

			C3-N7	$\pi^*$	0.26493	2.20	0.58	0.034
C10-H11	$\sigma$	1.93033	C3-N4	$\sigma^*$	0.09718	7.04	0.79	0.067
			N4-C10	$\sigma^*$	0.13167	3.55	0.78	0.048
			C10-H11	$\sigma^*$	0.06144	4.39	0.87	0.055
			C10-H12	$\sigma^*$	0.08768	7.57	0.84	0.071
C10-H12	$\sigma$	1.93648	C10-H11	$\sigma^*$	0.06144	5.34	0.80	0.058
			C10-H12	$\sigma^*$	0.08768	6.82	0.77	0.065
			C10-H13	$\sigma^*$	0.09592	5.26	0.83	0.059
C10-H13	$\sigma$	1.91973	C1-N4	$\sigma^*$	0.04015	7.37	0.83	0.070
			C3-N7	$\sigma^*$	0.02732	0.92	1.07	0.028
			N4-C10	$\sigma^*$	0.13167	4.09	0.78	0.051
			C10-H12	$\sigma^*$	0.08768	7.97	0.84	0.073
			C10-H13	$\sigma^*$	0.09592	5.05	0.90	0.060
LP(1)N4		1.58336	C1-C2	$\pi^*$	0.17529	17.57	0.31	0.070
			C1-N4	$\sigma^*$	0.04015	3.06	0.61	0.043
			C3-N4	$\sigma^*$	0.09718	3.01	0.57	0.040
			C3-N7	$\pi^*$	0.26493	24.07	0.28	24.07
			N4-C10	$\sigma^*$	0.13167	15.17	0.56	0.089
			C10-H12	$\sigma^*$	0.08768	5.12	0.62	0.055
LP(1)N7		1.93212	C1-C2	$\sigma^*$	0.01482	3.14	1.00	0.051
			C2-H6	$\sigma^*$	0.01340	0.89	0.83	0.025
			C3-N4	$\sigma^*$	0.09718	9.33	0.67	0.071
			C3-S8	$\sigma^*$	0.09363	0.84	0.53	0.019
LP(1)S8		1.96709	C3-N4	$\sigma^*$	0.09718	2.73	0.90	0.045
			C3-N7	$\sigma^*$	0.02732	1.19	1.18	0.033
			C3-N7	$\pi^*$	0.26493	3.10	0.61	0.041
			C10-H13	$\sigma^*$	0.09592	1.61	1.01	0.037
LP(2)S8		1.80847	C3-N4	$\sigma^*$	0.09718	5.15	0.55	0.049
			C3-N7	$\sigma^*$	0.02732	8.00	0.82	0.076
			C3-N7	$\pi^*$	0.26493	0.89	0.26	0.014
			C3-S8	$\sigma^*$	0.09363	16.20	0.41	0.075
			S8-H9	$\sigma^*$	0.03208	5.80	0.46	0.048
			C10-H13	$\sigma^*$	0.09592	9.75	0.66	0.073
C3-N7	$\pi^*$		C1-C2	$\pi^*$	0.17529	28.18	0.03	0.056
			C3-N4	$\sigma^*$	0.09718	0.54	0.30	0.026
			S8-H9	$\sigma^*$	0.03208	1.85	0.21	0.045
N4-C10	$\sigma^*$		C1-N4	$\sigma^*$	0.04015	0.81	0.05	0.019
			C10-H11	$\sigma^*$	0.06144	19.99	0.09	0.119
			C10-H12	$\sigma^*$	0.08768	62.00	0.06	0.163
			C10-H13	$\sigma^*$	0.09592	15.87	0.12	0.114

<sup>a</sup> E(2) means energy of hyper conjugative interaction (stabilization energy).

<sup>b</sup> E(i) E(j) Energy difference between donor and acceptor i and j NBO orbitals.

<sup>c</sup> F(i,j) is the Fock matrix element between i and j NBO orbitals.

i:donor orbital; j:acceptor orbital; a.u.: atomic unit; e:occupancy

### 3.4 Non-linear optical property analysis

Non-linear optics is one of the foremost areas of research today, and it provides vital contributions to emerging technologies in the fields of signal processing, telecommunications, and interconnections, as well as frequency switching, optical switching, optical logic, optical modulation, and optical memory. The dipole moment, polarizability, and first-order hyperpolarizability for the title molecule were calculated and are listed in **Table 4**. The high sensitivity of the hyperpolarizabilities to the basis set in work and the theoretical approach accepted leads to a change in the value of

hyperpolarizability due to the electron association. Organic molecules accommodated N-H groups enhanced their molecular hyperpolarizability and mechanical stabilities due to the hydrogen bond interaction<sup>15</sup>. Urea is the prototype molecule used to explore the NLO properties of the compound. For this reason, urea is often used as a threshold value for comparison purposes. The computed first-order hyperpolarizability of the compound is  $41.13903 \times 10^{-31}$  e.s.u and it is greater than the value of urea ( $\beta_0 = 0.372 \times 10^{-31}$  e.s.u). So, it is predicted to be a good NLO compound.

**Table 4.** The values of calculated dipole moment  $\mu$  (D), polarizability ( $\alpha$ ), first order hyperpolarizability ( $\beta_{tot}$ ) Methimazole compound. Calculated at B3LYP/6-311 ++ G (d, p) method.

Type of component	Methimazole
$\beta_{xxx}$	-195.8035559
$\beta_{xxy}$	-40.7240188
$\beta_{XYY}$	-24.1296165
$\beta_{yyy}$	54.2657788
$\beta_{xxz}$	19.428 5796
$\beta_{xyz}$	15.900351
$\beta_{yyz}$	122.9879005
$\beta_{xzz}$	-244.206387
$\beta_{yzz}$	-8.9766742
$\beta_{zzz}$	-53.9368211
$\beta_t$	$41.13903 \times 10^{-31}$
$\mu_x$	-0.087219
$\mu_y$	-0.4560474
$\mu_z$	-0.2756705
$\mu_t$	0.472425
$\alpha_{xx}$	94.6163166
$\alpha_{xy}$	0.6207925
$\alpha_{yy}$	107.223447
$\alpha_{xz}$	-9.5764742
$\alpha_{yz}$	2.0065636
$\alpha_{zz}$	65.5310923
$\Delta\alpha$	89.1236

However,  $\alpha$  and  $\beta$  values of the Gaussian output are in atomic units (a.u.), so they have been converted into electronic units (e.s.u.), ( $\alpha$ ; 1 a.u. =  $0.1482 \times 10^{-24}$  e.s.u.,  $\beta$ ; 1 a.u. =  $8.6393 \times 10^{-33}$  e.s.u.).

### 3.5 Molecular electrostatic potential map (MESP) analysis

MESP explains the charge density of the compounds in three dimensions. To explore the molecular interactions in any compound MESP is a vital one and it gives the negative and positive regions in the molecule that is nucleophilic and electrophilic attacking centers of the molecule<sup>16</sup>. The MEP  $V(r)$  at a point  $r$  is represented as:

$$V(r) = \sum^N \frac{Z_A}{|r - R_A|} - \int \rho(r') d^3 r' / |r - r'| \quad (2)$$

The MEP of the title molecule was calculated and the results are shown in **Fig. 4(a) & Fig. 4(b)**.

The MESP of molecules changes with different colors i.e., red, blue, green, and yellow, where red color shows the maximum negative regions of electrostatic potential, blue suggests positive electrostatic potential<sup>17</sup>. In Methimazole, the region around nitrogen atoms is more electronegative than around the N-methyl nitrogen atom, and oxygen atoms, the remaining region around hydrogen atoms of the molecule has positive electrostatic potential. This indicates that the negative potential region is electrophilic and the positive region potential region is nucleophilic for the molecules under investigation.

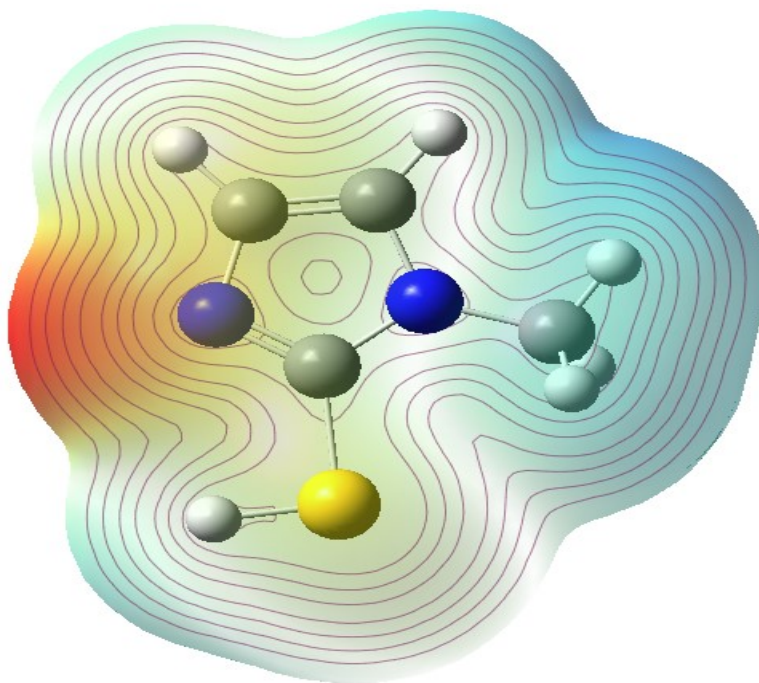


**Fig. 4(a).** Molecular electrostatic potential counter map for the Methimazole compound.

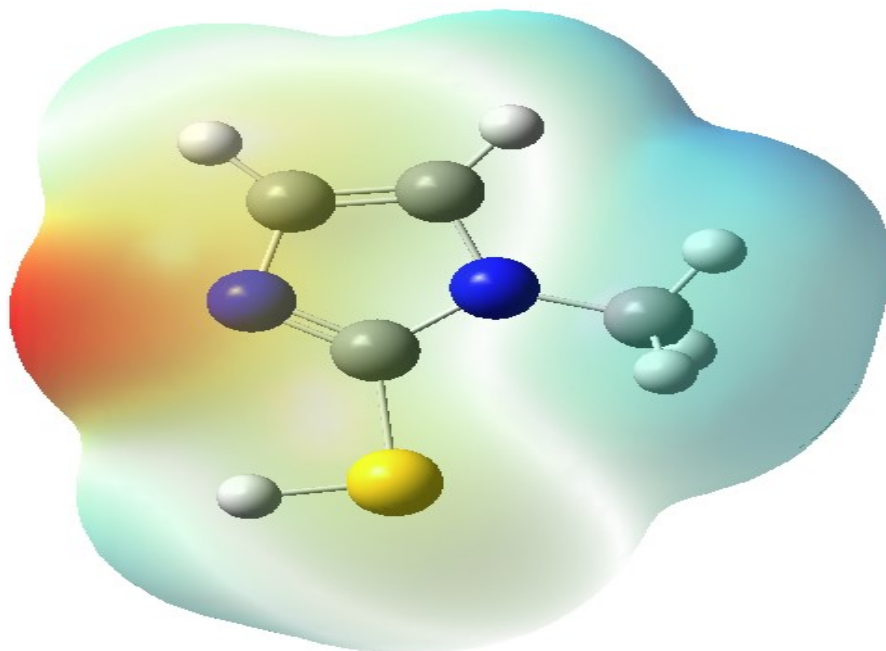


**Fig. 4(b).** Molecular electrostatic potential map for the Methimazole compound.

### 3.6. Chemical reactivity parameters:

Frontier molecular orbital (FMO) study estimates a significant parameter for quantum chemistry and determining the stability of the structure. It can be denoted as HOMO and LUMO<sup>18</sup>. HOMO can be considered as a nucleophile that donates electrons, and LUMO can consider an electrophile that accepts electrons from nucleophiles. By using DFT studies, the chemical reactivity of the header molecule can be explained by the calculation of some related parameters such as the energy gap (Eg), ionization energy (IP), electron affinity (EA), electronegativity ( $\chi$ ), chemical potential ( $\mu$ ), hardness ( $\eta$ ), global electrophilicity index ( $\omega$ ), softness ( $\sigma$ ), and dipole moment, respectively in the framework of Koopmans' theorem (equations 6-11)<sup>19</sup>.

$$IP = -E_{HOMO} \quad (3)$$

$$EA = -E_{LUMO} \quad (4)$$

Electronegativity ( $\chi$ ) can be specific to the molecule's ability to donate electrons and can also be determined as the inverse of chemical potential ( $\mu$ ).

The following properties are calculated as follows by using the energy gap value:

$$\mu = -(I+A)/2, \text{ (Chemical potential)} \quad (5)$$

$$\eta = (I-A)/2, \text{ (Chemical hardness)} \quad (6)$$

$$\sigma = 1/2\eta, \text{ (Chemical softness)} \quad (7)$$

$$\omega = \mu^2 / 2 \eta \text{ (Electrophilicity index)} \quad (8)$$

All these parameters were calculated for title at the B3LYP/6-311 ++G (d, p) basis set and shown in **Fig. 5**. The softness ( $\sigma$ ) and hardness ( $\eta$ ) are efficient handlings of the system's reactivity and electrophilicity index. Hardness is a standard for reducing energy due to the maximum electron circulation between the donors and acceptor units during the compound that deals with the escape propensity of electron clouds. The classification of a molecule, as hard and soft molecules potentially depends on the values of energy gaps. A large energy gap suggests that the compound is a hard molecule and a small HOMO-LUMO gap value designates that it is a soft molecule. For the

headline molecule, the HOMO-LUMO energy gap is 1.081925 eV. Reactivity and stability of a chemical system are related to its overall hardness. The stability was directly correlated to global hardness, and the reactivity is inverse<sup>20, 21</sup>. In our title molecule, the hardness is  $\eta = 0.549125\text{eV}$ , which shows that the molecule, possesses less stability and higher reactivity. In addition, finding the biological activity is also supplemented by the electrophilicity index ( $\omega$ ).

The theoretical calculation is displayed in **Table 5**. Also, electronegativity ( $\chi$ ) could be described as the electron donation ability of the molecule and can also be established as the negative of the chemical potential ( $\mu$ ). The chemical reactivity parameters analysis revealed that Methimazole is attractive, functional, and efficient and may be predicted as a possible descriptor of biological activities.

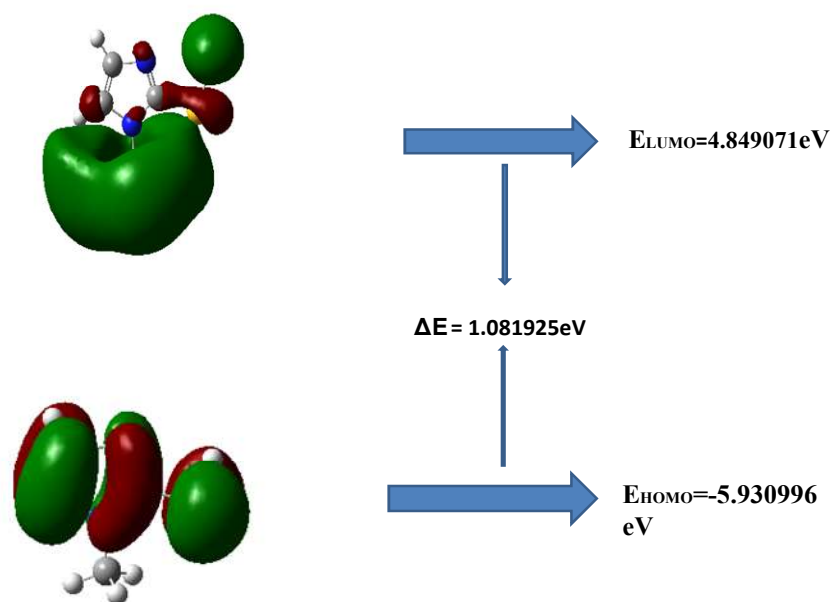


**Fig. 5.** Atomic orbital HOMO → LUMO composition of the frontier molecular orbital for Methimazole compound.

**Table 5.** Frontier molecular orbital properties for Methimazole

Quantum parameter	Methimazole
E(HOMO) / eV	-5.930996
E(LUMO) / eV	-4.849071
$\Delta E$ energy / eV	1.081925
Ionization energy, IP (eV)	5.930996
Electron affinity, EA (eV)	4.849071
Electronegativity, $\chi$ (eV)	-0.204497
Electrophilicity index( $\omega$ ) / (eV)	6.565455
Chemical Softness ( $\sigma$ ) / eV	-3.6421011
Chemical hardness( $\eta$ ) / eV	0.549125
Chemical potential ( $\mu$ )	-4.890033

eV: Electron Volt.

HOMO: Highest occupied molecular orbital

LUMO: Lowest unoccupied orbital

### 3.7 Mulliken atomic charges

Mulliken atomic charges play a pivotal role in the DFT calculations in optimized molecular geometry of the molecular structure, dipole moment, and electronic structure of molecule<sup>22-25</sup>. Mulliken atomic charges of atomic sites as shown in **Fig. 6** of Methimazole have been computed using the DFT/B3LYP/6-311 ++G (d, p) basis set and are collected in **Table 6** where it could be seen that the two carbon C2 and C8 atoms of Methimazole ring possess positive charges as 0.010534, and 0.001040 a.u., respectively, except

the C1 and C3 atom in **Fig. 6** bears negative charges as -0.012683 a.u. and -0.033983 a.u. due to SH group. Furthermore, the N4 atom shows a positive charge of 0.015447 and N7 possesses negative atomic charges of -0.035764 and a.u. for the site of respective atoms. Similar to the six hydrogen atoms, H5, H6, H9, H10, H11, and H13 of Methimazole possess Mulliken atomic charges as -0.000099, 0.000117, -0.002322, 0.000327, -0.000642, and 0.619437 a.u. to the respective atoms. Here, the S12 atom possesses high electronegativity as -0.160308.

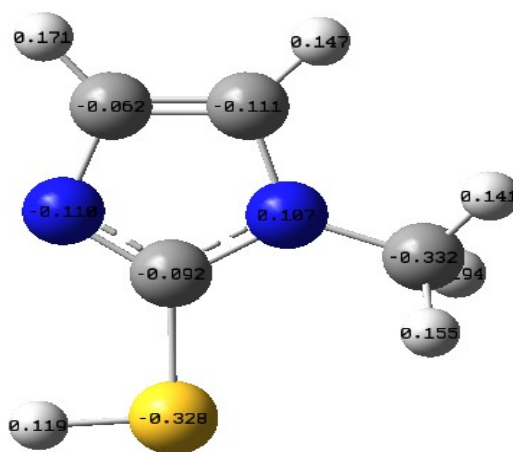


**Fig. 6.** Mulliken atomic charges of Methimazole

**Table 6.** Mulliken charges of Methimazole molecule with B3LYP/6- 311++G (d, p).

Atom	Mulliken charge	ATP charge
C 1	-0.012683	-0.049807
C 2	0.010534	0.057286
C3	-0.033983	0.535998
N4	0.015447	-0.385718
H5	-0.000099	0.082801
H6	0.000117	0.058784
N7	-0.035764	-0.551006
C8	0.001040	0.331047
H9	-0.002322	0.007219
H10	0.000327	0.014360
H11	-0.000642	-0.024529
S12	0.319560	-0.160308
H13	0.619437	0.083873

### 3.8 Drug likeness

Computational studies were useful to study the different physicochemical features of pharmacokinetic descriptors which were analyzed for the header molecule through the online tool Molinspiration Cheminformatics server. Drug likeness is the standard abstraction used for a drug-like property, which is described in the complex equilibrium of special molecular properties and structural property that calculates whether a specific molecule is related to known drugs. These molecular properties are generally hydrophobicity, electronic distribution, hydrogen bonding properties, and the existence of various pharmacological aspects that influence the molecular behavior of organisms, incorporating bioavailability, transport properties, interaction with proteins, reactivity, toxicity, metabolic stability, and many others.<sup>26</sup> Lipinski's rule of five was used to estimate the bioavailability of bulk materials to determine the drug-likeness properties; this rule plays a major role in drug discovery. In the present work, the physicochemical properties study of bulk molecules was implemented with the Molinspiration Cheminformatics program. The

drug-likeness of the Methimazole molecule was analyzed and presented in **Table 7**.

The drug-like element was deliberated by different parameters such as logP, molecular weight, number of heavy atoms, hydrogen donor, hydrogen acceptor, and rotatable bonds. Lipinski's rule is utilized to predict the drug-likeness properties and it is stated that the drug-likeness capability depends upon five significant factors: Log P values of compounds should have below 5, molecular weight less than 500, H-bond acceptors should be less than 10, H-bond donors should be less than 5 and bioactive scores should have less than one. The molecular weight of methimazole was 114.20 (less than 500), the number of H-bond donors and acceptors was one and three respectively and the bioactivity score is 0.55 and thus the title molecule has a good drug-likeness skill<sup>27</sup>. Log P: It is a major parameter, which is applied to predict the compound's hydrophobic character and it influences the absorbing tendency, bio-accessibility, stacking interaction between drug and receptor metabolism, and their toxicity problems. In the current research, logP values for methimazole 0.7088, signify that the material must have moderate penetrable talent in the central nervous system.

**Table 7.** Drug-likeness properties of Methimazole.

Molecular formula	C <sub>4</sub> N <sub>2</sub> SH <sub>6</sub>
Molecular weight(g/mol)	114.20
log P	0.7088
TPSA (Å <sup>2</sup> )	17.83
No. of H bond acceptor	3
No. of H bond donars	1
No. of rotatable bonds	0
Bioactivity score	0.55
Toxicity	None

### 3.9. *In silico* pharmacokinetics ADMET and drug likeness prediction

The employ of computational techniques to determine the new candidate drugs assist to reduce the number of experimental studies and improving the success rate. For this reason, we

used the ADMET (adsorption, distribution, metabolism, excretion, and toxicity) profile for a measure of pharmacokinetics parameters<sup>28</sup>. The title compound predicted by the 2D-QSAR model has almost the same activities. The pkCSM online tool was employed to predict *in silico* ADMET properties. From **Table 8**, an absorbance value

below 30% indicates poor absorbance, which shows poor absorbance in the human intestine. The volume of distribution (VDss) is considered high if the value is greater than 0.45. Moreover, blood-brain barrier (BBB) and central nervous system (CNS) permeability standard values ( $>0.3$  to  $<-1$  log BB and  $>-2$  to  $<-3$  log PS, respectively) were obtained. For a given compound, log BB  $<-1$  means that the drug is poorly distributed to the brain, while log BB  $> 0.3$  means that it has the potential to cross the BBB, and log PS  $>-2$  means that it can penetrate the CNS, while log PS  $<-3$  means that it is difficult for the drug to move into the CNS. The results indicated that title compounds presented a significant potential to cross the barriers. The metabolism suggested the chemical biotransformation of a drug by the body. Drugs thus produce a variety of metabolites, each of which may have unique physicochemical and pharmacological characteristics. It is required to consider the metabolism of drugs and drug-drug interactions. Cytochrome P450 (CYP450) plays a critical role in drug metabolism because the major liver enzyme system is involved in phase I

metabolism (oxidation), as was the case of our study. Until CYP groups have been identified in humans, although only CYP1, CYP2, CYP3, and CYP4 are involved in drug metabolism, with CYP (1A2, 2C9, 2C19, 2D6, and 3A4) being responsible for the biotransformation of more than 90% of drugs undergoing phase I metabolism. Moreover, cytochrome CYP3A4 inhibition is the mainly important phenomenon in this study. Moreover, the title compound was found to be the substrate of CYP3A4 and the inhibitor of CYP3A4. Clearance is a constant that describes the relationship between the drug concentration in the body and the rate of elimination of the drug. Therefore, a low value of total clearance means increased persistence of drugs in the body, and compounds show good persistence of the drug in the body. In addition, it is necessary to examine whether the predicted compounds are non-toxic because this plays a critical role in the selection of drugs. According to these results, it can be concluded that the compound is used as a drug against the thyroid.

**Table 8.** In silico ADMET prediction of Methimazole compound.

Absorption	Distribution			Metabolism						Excretion	Toxicity
	Intestinal absorption (human)	BBB permeability	VDss	CNS Permeability	Substrate Inhibitor						
CYP											
Numeric (% absorbed)	Numeric (log L kg <sup>-1</sup> )	Numeric (log BB)	Numeric (log PS)	Inhibitor			Substrate			Numeric (log ml.min <sup>-1</sup> . kg <sup>-1</sup> )	Categorical (yes/no)
				Categorical (yes/no)							
30	-0.265	-0.353	-2.855	2C19	2C9	2D6	3A4	2D6	3A4	0.797	No
				No	Yes	No	Yes	No	Yes		

### 3.10 Molecular docking

The binding abilities of the title molecule were examined using the molecular docking approach. Thus we selected the target macromolecule for docking simulation. The high-resolution 3D crystal structure of (PDB ID: 1NHZ) was downloaded from the Protein Data Bank website.

All molecular docking calculations were performed on Auto Dock 4.2 software<sup>29</sup>. The protein was prepared for docking by removing the co-crystallized ligands, waters, and cofactors. Calculations of Kollman charges and polar hydrogens were performed using the Auto Dock Tools (ADT) graphical user interface. The ligand was prepared for docking by minimizing its

energy at the B3LYP level of theory. Partial charges were calculated by the Geistenger method. The active site of the enzyme was defined to include residues of the active site within the grid size of 40 Å X40 Å X 40 Å. The docking protocol was tested by extracting a co-crystallized inhibitor from the protein and then redocking the same. Amongst the docked conformations of the title ligand, one which binds well at the active site was analyzed for detailed

interactions in Discover Studio Visualizer 4.0 software. The ligand binds at the active site of the substrate (Fig. 7(a) & 7(b)) by weak non-covalent interactions. THR-739 amino acid forms an H-bond with the SH group of methimazole. The docked ligand title compound forms a stable complex with anti-thyroid protein giving a binding affinity value of -2.33 kcal/mol (Table 9). These preliminary results suggest that the compound might exhibit anti-thyroid.

**Table 9.** Docking and hydrogen bond interaction of target molecule with different proteins.

Protein (PDB ID)	Bonded Residues	No. of hydrogen bonds	Estimated inhibition constant( $\mu\text{m}$ )	Binding energy (kcal/mol)	Reference RMSD
1NHZ	THR739	1	19.66	-2.33	26.21

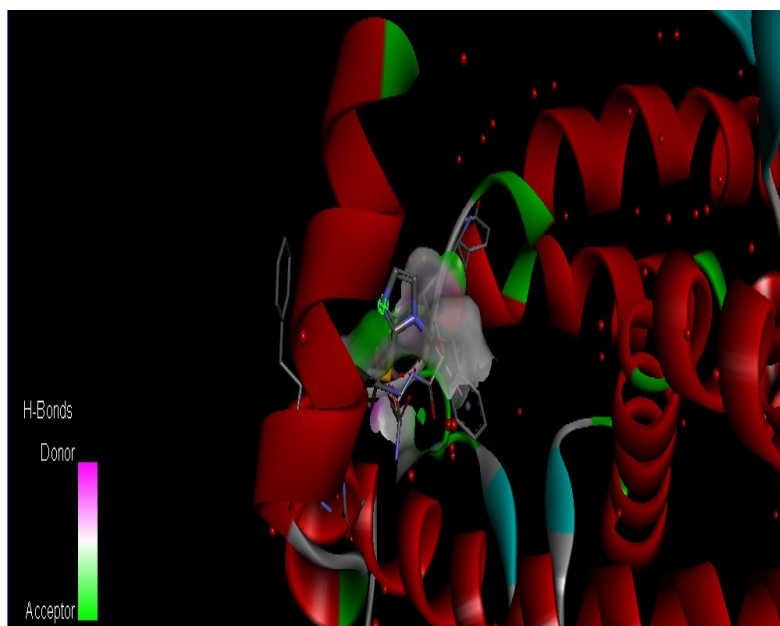


**Fig. 7(a).** Docking and hydrogen bond interactions of Methimazole compound with 1NHZ protein structure.

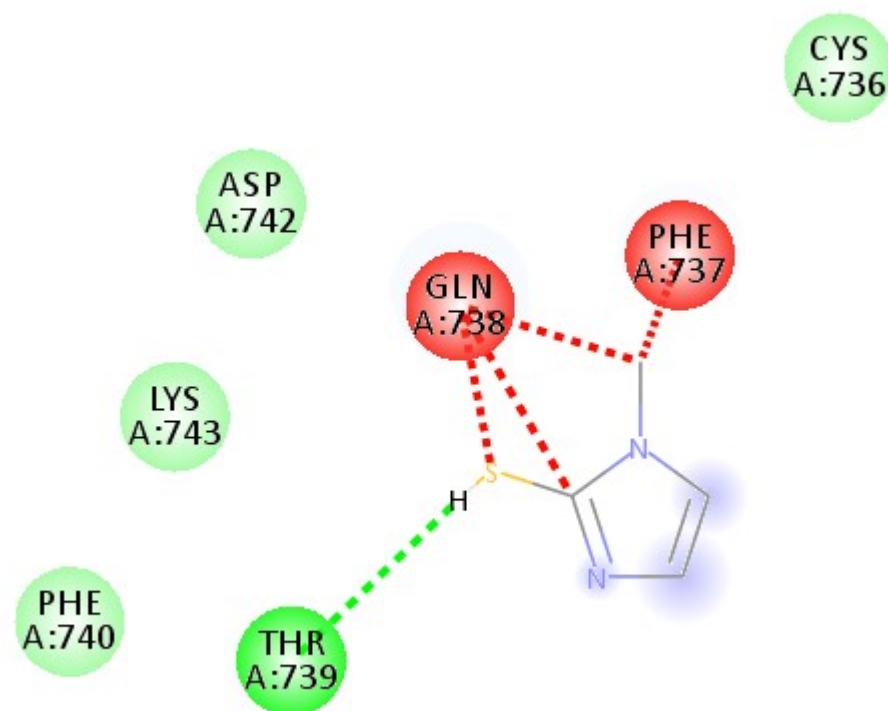


**Fig.7(b).** Hydrogen bond interactions of Methimazole compound with 1NHZ protein structure.

#### 4. Conclusion

The optimized conformation, IR, and vibrational assignments of MTZ have been carried out using the DFT calculation with B3LYP/6 - 311++G (d, p) basis set. The molecule's intermolecular and hyper conjugative contacts were calculated using NBO analysis, and the structure's stability indicated that the  $\sigma$  of N4-C10 to  $\sigma^*$ C10-H12, interactions is 62.0 kcal/mol would contribute the most to stabilization energy. The calculated HOMO and LUMO energy gap ( $E_{\text{gap}} = 1.081925$  eV) value of the headline compound is comparable with drug molecules. The MEP map shows a biologically active region of the headline compound around N-methyl nitrogen atom and oxygen atoms in negative potential sites. Drug likeness values show the title compound has no violation to be used as a drug; importantly Lipinski's rule of five is satisfied with title molecule. Finally, a molecular docking study confirmed the drug nature of the title compound through H-bond interactions and minimum binding energy. THR-739 amino acid forms an H-bond with the SH group of methimazole. Hence from all the above the studies title compound shows biologically active and drug nature within

the molecule. So, after experimental and clinical research this compound might be used as a potential drug.

#### References

1. C. Laurence, M.J. El Ghomari, M. Lucon, "Structure and molecular interactions of anti-thyroid drugs. Part 1. Dipole moments of carbimazole and methimazole, and conformation of carbimazole," *J. Chem. Soc., PerkinTrans. 2*, no.05 (1998): 1159-62. <https://doi.org/10.1039/A800621K>.
2. C. Laurence, M.J. El Ghomari, J.-Y. Le Questel, M. Berthelo, R. Mokhlisse, "Structure and molecular interactions of anti-thyroid drugs. Part 3.1 Methimazole: a diiodine sponge," *J. Chem. Soc., Perkin Trans. 2*, no. 07 (1998): 1545-52. <https://doi.org/10.1039/A803002B>.
3. R. Subramanian, V. Lakshminarayanan, "Effect of adsorption of some azoles on copper passivation in alkaline medium," *Corros. Sci.* 44 (2002): 535-54. [https://doi.org/10.1016/S0010-938X\(01\)00085-3](https://doi.org/10.1016/S0010-938X(01)00085-3).
4. J.Y. Sun, C.Y. Zheng, X.L. Xiao, L. Niu, T.Y. You, E.K. Wang, "Electrochemical detection of methimazole by capillary electrophoresis at a carbon fiber microdisk electrode,"

- Electroanalysis* 17 (2005): 1675-80. <https://doi.org/10.1002/elan.200403272>.
5. X. Liao, Y. Chen, M. Qin, Y. Chen, H. Zhang, Y. Tian, "Au-Ag-Au double shell nanoparticles-based localized surface plasmon resonance and surface-enhanced Raman scattering biosensor for sensitive detection of 2-mercapto-1-methylimidazole," *Talanta* 117 (2013): 203-8. <https://doi.org/10.1016/j.talanta.2013.08.051>.
  6. D.L. Poster, M.M. Schantz, L.C. Sander, S.A. Wise, "Analysis of polycyclic aromatic hydrocarbons (PAHs) in environmental samples: a critical review of gas chromatographic (GC) methods," *Anal. Bioanal. Chem.* 4 (2006): 859-81. <https://doi.org/10.1007/s00216-006-0771-0>.
  7. K. A. Woeber, "Methimazole-Induced Hepatotoxicity," *Endocr. Pract.* 8, no.03 (2002): 222-4. <https://doi.org/10.4158/EP.8.3.222>.
  8. M. Garner, D. R. Armstrong, J. Reglinski, W. E. Smith, R. Wilson and J. H. McKillop, "The structure of methimazole and its consequences for current therapeutic models of graves' disease," *Bioorg. Med. Chem. Lett.*, 4, no. 11(1994): 1357-60. [https://doi.org/10.1016/S0960-894X\(01\)80361-9](https://doi.org/10.1016/S0960-894X(01)80361-9).
  9. R. Heidari, H. Babaei, L. Roshangar and M. A. Eghbal, "Effects of Enzyme Induction and/or Glutathione Depletion on Methimazole-Induced Hepatotoxicity in Mice and the Protective Role of N-Acetylcysteine," *Adv.Pharm. Bull.*, 4, no.01 (2014): 21-8. <http://dx.doi.org/10.5681/apb.2014.004>.
  10. A.D. Becke, "Densityfunctional thermochemistry. I. The effect of the exchangeonly gradient correction," *J. Chem. Phys.* 96, no.03 (1992): 2155-160. <https://doi.org/10.1063/1.462066>.
  11. C. Lee, W. Yang, P.G. Parr, "Development of the Colle-Salvetti correlation-energy formula into a functional of the electron density," *Phys. Rev. B* 37 no.02, (1988): 785-89. <https://doi.org/10.1103/PhysRevB.37.785>.
  12. S. Bangaru, P. Manivannan, S. Muthu, Spectroscopic investigations, quantum chemical calculations and molecular docking studies of Mangiferin—An anti-viral agent of H1N1 Influenza virus, *Chem. Data Collect.* 30 (2020) 100580, doi: 10.1016/j.cdc.2020.100580
  13. S. Aayisha, T.S. Renuga Devi, S. Janani, S. Muthu, M. Raja, R. Hema- malini, Structural (PES), AIM, spectroscopic profiling (FT-IR, FT-Raman, NMR and UV), HOMO → LUMO and docking studies of 2,2-dimethyl-N-(2-pyridinyl) propanamide—A DFT approach, *Chem. Data Collect.* 24 (2019) 100287, doi: [10.1016/j.cdc.2019.100287](https://doi.org/10.1016/j.cdc.2019.100287).
  14. E. D. Glendening, A. E. Reed, J. E. Carpenter, and F. Weinhold. NBO Version 3.1, TCI, University of Wisconsin, Madison, 1998. [https://doi: 10.4236/jssm.2017.103018](https://doi.org/10.4236/jssm.2017.103018)
  15. H. Sekina, R.J. Bartlett, "Hyperpolarisabilities of the hydrogen fluoride molecule: a discrepancy between theory and experiment," *J. Chem. Phys. Lett.* 84, no.5, (1986): 2726-33. <https://doi.org/10.1063/1.450348>.
  16. P. Politzer and D. G. Truhlar (Eds.), "Chemical Applications of Atomic and Molecular Electrostatic Potentials: Reactivity, Structure, Scattering, and Energetics of Organic, Inorganic and Biological Systems," (New York: Plenum Press, 1981). DOI <https://doi.org/10.1007/978-1-4757-9634-6>.
  17. T. E. Scrocco, "Electronic Molecular Structure, reactivity and intermolecular Forces: An Euristic Interpretation by Means of Electrostatic Molecular Potentials," *Journal of Advanced Quantum Chemistry* 11, (1978): 115-93. <https://doi.org/10.1016/j.heliyon.2022.e10122>.
  18. P. Politzer and K. C. Daiker, "Models for chemical reactivity, in *The Force Concept in Chemistry*," edited by B. M. Deb (New York: Van Nostrand Reinhold, 1981). <https://doi.org/10.1007/978-1-4757-9634-6-1>.
  19. M.R. Elmorsy, E. Abdel-Latif, S.A. Badawy, A.A. Fadda, "Molecular geometry, synthesis and photovoltaic performance studies over 2-cyanoacetanilides as sensitizers and effective cosensitizers for DSSCs loaded with HD-2," *J. Photochem. Photobiol. A. Chem.* 389, (2020):112239. <https://doi.org/10.1016/j.jphotochem.2019.112239>.
  20. K. Periyasamy, P. Sakthivel, P. Vennila, P.M. Anbarasan, G. Venkatesh, Y.S. Mary, "Novel D-π-A phenothiazine and dibenzofuran organic dyes with simple structures for efficient dyesensitized solar cells," *Journal of Photo Chemistry and Photobiology A: Chemistry*, 413, (2021): 113269.

- <https://doi.org/10.1016/J.JPHOTOCHEM.2021.113269>.
21. Z. Xu , Y. Li , W. Zhang , S. Yuan , L. Hao , T. Xu , X. Lu, “DFT/TD-DFT study of novel T shaped phenothiazine-based organic dyes for dye-sensitized solar cells applications,” *Spectrochim. Acta Part A* 212 (2019): 272-280. <https://doi.org/10.1016/j.saa.2019.01.002>.
  22. M.M.C. Ferreira, E. Suto, “Atomic Polar Tensor Transferability and Atomic Charges for the Fluoromethane Series CH<sub>x</sub>F<sub>4-x</sub>,” *The Journal of Physical Chemistry* 96, no.22, (1992): 8844-49. <https://doi.org/10.1021/j100201a030>.
  23. M.J.S. Dewar, *The Molecular Orbital Theory of Organic Chem* (Mc. GrawHill and Inc., New York, 1969). <https://doi.org/10.1002/ange.19700820418>.
  24. C.A. Coulson, R. McWeeny, *Coulson's Valence* (Oxford University Press, Oxford, 1979).
  25. M.J. Frisch et al., *Gaussian 09, Revision C.01* (G. Inc., Wallingford, 2010) <https://doi.org/10.1039/C3CC42593B>.
  26. C. A. Lipinski, F. Lombardo, B. W. Dominy, and P. J. Feeney, “Experimental and Computational Approaches to Estimate Solubility and Permeability in Drug Discovery and Development Settings,” *Advanced Drug Delivery Reviews* 46, no. 1-3 (2001): 3-25. [https://doi.org/10.1016/s0169-409x\(00\)00129-0](https://doi.org/10.1016/s0169-409x(00)00129-0).
  27. L. L. G. Ferreira and A. D. Andricopulo, “ADMET modeling approaches in drug discovery,” *Drug Discovery Today* 24, no.05 (2019): 1157-65. <https://doi.org/10.1016/j.drudis.2019.03.015>.
  28. D. E. Clark, “In silico prediction of Blood-Brain-Barrier permeation,” studies of *Drug Discovery Today* 8, no.20 (2003): 927-33. [https://doi.org/10.1016/s1359-6446\(03\)02827-7](https://doi.org/10.1016/s1359-6446(03)02827-7).
  29. G.M. Morris, R. Huey, W. Lindstrom, M.F. Sanner, R.K. Belew, D.S. Goodsell, A.J. Olson, AutoDock4 and AutoDockTools4: Automated docking with selective receptor flexibility, *J. Comput. Chem.* 30 (16) (2009) 2785-2791. DOI: [10.1002/jcc.21256](https://doi.org/10.1002/jcc.21256).

Access this Article in Online	
	Website: <a href="http://www.ijcrps.com">www.ijcrps.com</a>
	Subject: Chemistry
Quick Response Code	
DOI: <a href="https://doi.org/10.22192/ijcrps.2025.12.06.001">10.22192/ijcrps.2025.12.06.001</a>	

How to cite this article:

Natte kavitha, Munagala Alivelu, Macha Bhavani, Samaleti Priyanka. (2025). Exploring Methimazole by Spectroscopic, NLO, NBO, ADME Analysis, and Molecular Docking Studies using the DFT method. *Int. J. Curr. Res. Chem. Pharm. Sci.* 12(6): 1-19.  
DOI: <http://dx.doi.org/10.22192/ijcrps.2025.12.06.001>